Gen Relativ Gravit (2009) 41:1125–1137
DOI 10.1007/s10714-008-0694-5

RESEARCH ARTICLE

Cosmological model with interactions in the dark sector

Luis P. Chimento · Mónica Forte · Gilberto M. Kremer

Received: 26 April 2008 / Accepted: 9 September 2008 / Published online: 20 September 2008

Abstract A cosmological model for the present Universe is analyzed whose constituents are a non-interacting baryonic matter field and interacting dark matter and dark energy fields. The dark energy and dark matter are coupled through their effective barotropic indexes, which are considered as functions of the ratio of their energy densities. Two asymptotically stable cases are investigated for the ratio of the dark energy densities which have their parameters adjusted by considering best fits to Hubble function data. It is shown that the deceleration parameter, the density parameters, and the luminosity distance have the correct behavior which is expected for a viable present scenario of the Universe.

Keywords Dark energy · Dark matter · Interacting fluids

1 Introduction

Recent observations of Supernova Ia (SNIa) suggest that the Universe has entered into a stage of an accelerated expansion with a redshift $z \lesssim 1$ [1–4]. This has been confirmed by precise measurements of the spectrum of the cosmic microwave background (CMB) anisotropies [5,6] as well as the baryon acoustic oscillations (BAO) in the Sloan digital

L. P. Chimento · M. Forte
Departamento de Física, Facultad de Ciencias Exactas y Naturales, Universidad de Buenos Aires, Ciudad Universitaria, Pabellón I, 1428 Buenos Aires, Argentina
e-mail: chimento@df.uba.ar

M. Forte
e-mail: forte.monica@gmail.com

G. M. Kremer (✉)
Departamento de Física, Universidade Federal do Paraná,
Caixa Postal 19044, Curitiba 81531-990, Brazil
e-mail: kremer@fisica.ufpr.br

sky survey (SDSS) luminous galaxy sample [7]. All usual types of matter with positive pressure generate attractive forces and decelerate the expansion of the universe. For that reason, a dark energy component with negative pressure was suggested to account for a fluid that drives the current accelerated expansion (see [8–13] for reviews). The simplest explanation of dark energy is provided by a cosmological constant, but the scenario is plagued by a severe fine tuning problem associated with its energy scale. The vacuum energy density falls below the value predicted by any sensible quantum field theory by many orders of magnitude [14], and it unavoidably leads to the coincidence problem, i.e.,"Why are the vacuum and matter energy densities of precisely the same order today?" [15]. More sophisticated models replace the cosmological constant by a dynamical dark energy that may be a scalar field (quintessence), tachyon field, phantom field or exotic equations of state. These models fit the observational data but it is doubtful that they can solve the coincidence problem [16,17]. Besides, in a viable dark energy scenario we require that the energy density of the dark fluid remains subdominant during radiation and matter dominant eras and that it becomes important only at late times to account for the current acceleration of the Universe.

In several papers, it has been proposed that dark matter and dark energy are coupled and do not evolve separately [18–33]. The coupling between matter and quintessence is either motivated by high energy particle physics considerations [26] or is constructed by requiring the final matter to dark energy ratio to be stable against perturbations [17,35]. In the same sense, we will use two arbitrary interacting fluids in the dark sector, with constant barotropic indexes, and will show that there is a stable solution for the ratio dark matter-dark energy, which satisfies the expected behavior from the matter dominated era until today.

The present paper differs from the majority of the works in the literature on dark energy–dark matter interactions in two main points, namely, (i) the baryon field is treated separately from the dark matter field and is considered as a non-coupled field and (ii) the dark energy and dark matter energy transfer is proportional to the dark energy density. This last assumption is very important, since in a recent paper Pavón and Wang [34] showed that the coupling proportional to the dark energy density is the only that satisfies the second law of thermodynamics and the principle of Le Châtelier.

We explain in Sect. 2 the general features of the model for two different interactions and find the stability conditions of the ratio dark matter–dark energy. The Sect. 3 is devoted to obtain the values of parameters that best fit the observational data using the recently published Hubble function $H(z)$ data [36], extracted from differential ages of passively evolving galaxies. The allowed regions of probability 1σ and 2σ for the parameters are shown. Also, deceleration parameter, density parameters, ratio dark matter–dark energy, effective equations of state and luminosity distance are exhibited in Sect. 4 for the best fit parameters, showing the correct behavior expected for a viable scenario. Finally, in Sect. 5 we compare our model with some existing models on dark matter–dark energy interaction and present our conclusions.

2 Interacting dark model

Let us consider a Universe modeled by a mixture of three constituents, namely, baryons, dark matter and dark energy. The Friedmann and energy conservation equations read

$$3H^2 = \rho_1 + \rho_2 + \rho_3, \tag{1}$$

$$\dot{\rho}_1 + \dot{\rho}_2 + 3H(\rho_1 + p_1 + \rho_2 + p_2) = 0, \tag{2}$$

$$\dot{\rho}_3 + 3H(\rho_3 + p_3) = 0. \tag{3}$$

respectively. The subindexes 1 and 2 refer to dark matter and dark energy, respectively, whereas the subindex 3 to baryons. The baryonic matter is supposed to be a noninteracting component so that it decouples from equation (2). Moreover, by considering the baryons as pressureless ($p_3 = 0$), the integration of equation (3) gives $\rho_3 = \rho_3^0 (a_0/a)^3$, where ρ_3^0 and a_0 represent the present values of the energy density and cosmic scale factor, respectively. In the above equations the dot represents derivative with respect to time and $H = \dot{a}/a$ is the Hubble parameter.

Hence, Eq. (2) expresses the interaction between the dark matter and dark energy allowing the mutual exchange of energy and momentum. Consequently, there will be no local energy–momentum conservation for the fluids separately. However, we can decouple Eq. (2) into two "effective equations of conservation" as follows

$$\dot{\rho}_1 + 3H\gamma_1^e \rho_1 = 0, \tag{4}$$

$$\dot{\rho}_2 + 3H\gamma_2^e \rho_2 = 0. \tag{5}$$

In the above equations it was introduced effective barotropic indexes γ_i^e ($i = 1, 2$) given by

$$\gamma_1^e = \gamma_1 + \frac{\gamma_2}{r} + \frac{\dot{\rho}_2}{3H\rho_1}, \tag{6}$$

$$\gamma_2^e = \gamma_2 + \gamma_1 r + \frac{\dot{\rho}_1}{3H\rho_2}, \tag{7}$$

where $r = \rho_1/\rho_2$ is the ratio of the energy densities and γ_i ($i = 1, 2$) represent barotropic indexes of the equations of state $p_i = (\gamma_i - 1)\rho_i$.

In addition we get the relationship

$$(\gamma_1^e - \gamma_1)r + (\gamma_2^e - \gamma_2) = 0, \tag{8}$$

and a dynamical equation for the ratio r, namely

$$\dot{r} = -3Hr\Delta\gamma^e, \quad \Delta\gamma^e = \gamma_1^e - \gamma_2^e. \tag{9}$$

We assume that the effective barotropic index of the dark energy is given by $\gamma_2^e = \gamma_2 - F(r)$, where $F(r)$ is a function which depends on the ratio r, so that we get

$$\Delta\gamma^e = \Delta\gamma + F(r)\left(1 + \frac{1}{r}\right), \quad \Delta\gamma = \gamma_1 - \gamma_2. \tag{10}$$

By taking into account the above representation for γ_2^e, Eqs. (4) and (5) can be rewritten as

$$\dot{\rho}_1 + 3H\rho_1\gamma_1 = -3H\rho_2 F(r), \tag{11}$$

$$\dot{\rho}_2 + 3H\rho_2\gamma_2 = 3H\rho_2 F(r). \tag{12}$$

Now it is possible to identify the right-hand side of each above equations as the energy transfer between dark matter and dark energy.

Now we make a detailed study of the general dynamics of the density ratio r as given by Eq. (9) along with Eq. (10). To this end we assume that the constant solutions $r = r_s$, represent a stationary stage of the Universe. Then, according to Eq. (9), it means that $\Delta\gamma^e(r_s) = 0$. Then, the constant solutions r_s will be asymptotically stable whether $(d\Delta\gamma^e/dr)_{r=r_s} > 0$. Expressing this condition in terms of Eq. (10), we obtain the stability condition

$$r_s\,(1 + r_s)\left(\frac{dF}{dr}\right)_{r=r_s} - F(r_s) > 0, \tag{13}$$

where we have assumed that the barotropic indexes γ_i of the two fluids are constants. Note that the simplest choice, a negative constant F, satisfies the latter condition. This fact, induce us to investigate the F constant case. So, in the next sections we shall analyze two different choices for the function $F(r)$, namely, one refers to a constant and another being a variable.

2.1 $F(r) = \text{constant} < 0$

If we choose the barotropic indexes γ_1 and γ_2 as constants and the function $F(r)$ as

$$F(r) = -\frac{r_\infty}{1 + r_\infty}\Delta\gamma, \tag{14}$$

where r_∞ is a constant value of the ratio of the energy densities at infinity, then it is possible to integrate the Eq. (9) for r along with the effective conservation equations (4) and (5) for the energy densities, yielding

$$\rho_1 = \rho_2^0\left\{r_\infty + (r_0 - r_\infty)\left(\frac{a_0}{a}\right)^{3\alpha}\right\}\left(\frac{a_0}{a}\right)^{\beta}, \tag{15}$$

$$\rho_2 = \rho_2^0\left(\frac{a_0}{a}\right)^{\beta}, \tag{16}$$

where a_0 and r_0 are the present values of the cosmic scale factor and of the ratio of the energy densities, whereas

$$\alpha = \frac{\Delta\gamma}{1 + r_\infty}, \quad \beta = 3\frac{r_\infty\gamma_1 + \gamma_2}{1 + r_\infty}. \tag{17}$$

As usual we introduce the red-shift $z = 1/a - 1$ and the density parameters at the present value $z_0 = 0$, namely

$$\Omega_1^0 = r_0\Omega_2^0, \quad \Omega_2^0 = \frac{\rho_2^0}{3H_0^2}, \quad \Omega_3^0 = \frac{\rho_3^0}{3H_0^2}, \tag{18}$$

with $\Omega_1^0 + \Omega_2^0 + \Omega_3^0 = 1$. Once the explicit dependence of the energy densities are known in terms of the red-shift we can rewrite the Friedmann equation (1), thanks to (15) and (16), as

$$H^2 = H_0^2 \left\{ \Omega_2^0(1 + r_\infty)(1 + z)^\beta + \Omega_3^0(1 + z)^3 + [1 - \Omega_3^0 - (1 + r_\infty)\Omega_2^0](1 + z)^{3\gamma_1} \right\}, \tag{19}$$

which gives the dependence of the Hubble parameter H with respect to the red-shift.

2.2 Variable $F(r)$

One possible choice for the function $F(r)$ is

$$F(r) = -\frac{(1 - r)r_\infty^2}{r(1 - r_\infty^2)}\Delta\gamma, \tag{20}$$

where r_∞ has the same meaning as in the previous case. Note that the above chosen function reduces to (14) in the limit $r = r_\infty$. With this restriction the latter function satisfies the stability condition (13). So that, the stationary solution of Eq. (9), corresponding to the function (20), is asymptotically stable.

In this case the solution of Eqs. (4) and (5) are given by

$$\rho_1 = \rho_2^0 \sqrt{r_\infty^2 + (r_0^2 - r_\infty^2)\left(\frac{a_0}{a}\right)^\nu} \left(\frac{a_0}{a}\right)^{3\epsilon} \left[\frac{(1 - r/r_\infty)(1 + r_0/r_\infty)}{(1 - r_0/r_\infty)(1 + r/r_\infty)}\right]^{\frac{r_\infty}{2}}, \tag{21}$$

$$\rho_2 = \rho_2^0 \left(\frac{a_0}{a}\right)^{3\epsilon} \left[\frac{(1 - r/r_\infty)(1 + r_0/r_\infty)}{(1 - r_0/r_\infty)(1 + r/r_\infty)}\right]^{\frac{r_\infty}{2}}, \tag{22}$$

where

$$\nu = \frac{6\Delta\gamma}{1 - r_\infty^2}, \qquad \epsilon = \gamma_2 - \frac{\Delta\gamma r_\infty^2}{1 - r_\infty^2}. \tag{23}$$

Furthermore, the Hubble parameter H can be expressed as functions of the red-shift, yielding

$$\frac{H^2}{H_0^2} = \Omega_2^0(1 + z)^{3\epsilon} \left[\frac{(1 - r/r_\infty)(1 + r_0/r_\infty)}{(1 - r_0/r_\infty)(1 + r/r_\infty)}\right]^{\frac{r_\infty}{2}} \times \left\{1 + \sqrt{r_\infty^2 + (r_0^2 - r_\infty^2)(1 + z)^\nu}\right\} + \Omega_3^0(1 + z)^3. \tag{24}$$

Here it is interesting to call attention that the condition $r_\infty = 0$ leads to a mixture of noninteracting fluids with constant barotropic indexes for both cases analyzed above.

3 Cosmological constraints

The aim of this section is to determine the parameters (r_∞, β) for the constant $F(r)$ case and (r_∞, γ_2) for the variable $F(r)$ one. These parameters, denoted generically by a_i, are established through the recently published Hubble parameter $H(z)$ data [36], extracted from differential ages of passively evolving galaxies. This $H(z)$ function is a very interesting one, because in contrast to standard candle luminosity distances or standard ruler angular diameter distances, it is not integrated over. The Hubble parameter depends on the differential age of the Universe as a function of z in the form $H(z) = -(1+z)^{-1}dz/dt$, and it can be measured directly through a determination of dz/dt. In the procedure of calculating the differential ages, Simon et al. [36] have employed the new released Gemini Deep Deep Survey [37] and archival data [38,39] to determine the nine numerical values of $H(z)$ in the range $0 < z < 1.8$.

The probability distribution for the parameters a_1, a_2 is (see e.g. [40])

$$P(a_1, a_2) = \mathcal{N} e^{-\chi^2(a_1,a_2)/2},$$
$$\chi^2(a_1, a_2) = \sum_{i=1}^{9} \frac{[H_{th}(a_1, a_2; z_i) - H_{ob}(z_i)]^2}{\sigma(z_i)^2}, \tag{25}$$

where $\mathcal{N}$ is a normalization constant, $H_{ob}(z_i)$ is the observed value of H at the red-shift z_i, $\sigma(z_i)$ is the corresponding 1σ uncertainty, and the summation is over the nine observational $H(z_i)$ data points at red-shift z_i [36].

We adopt the values $H_0 = 72$ km s^{-1} Mpc^{-1} (mean value of the results from the Hubble Space Telescope key project), $\Omega_1^0 = 0.25$, $\Omega_2^0 = 0.70$ and $\Omega_3^0 = 0.05$ [41] and minimize this χ^2 function to obtain the values a_{1bf} and a_{2bf} that correspond to a maximum value of (25). Furthermore, we assume a spatially flat Universe with a pressureless (dust) dark matter, i.e., $\gamma_1 = 1$. Besides, we take the theoretical expressions for the Hubble parameter H_{th} with parameters $a_1 = r_\infty$, $a_2 = \beta$ in the F constant case and $a_1 = r_\infty$ and $a_2 = \gamma_2$, in the F variable case.

The best fit parameters a_{1bf} and a_{2bf} are obtained so that $\chi^2_{min}(a_{1bf}, a_{2bf})$ corresponds to the minimum of $\chi^2(a_1, a_2)$. If $\chi^2_{min}(a_{1bf}, a_{2bf})/(N-n) \leq 1$ the fit is good and the data are consistent with the considered model $H(z; a_1, a_2)$. Here, N is the range of data set used and n is the number of parameters [40].

The variable χ^2 is a random variable in the sense that it depends on the random data set used. Its probability distribution is a χ^2 distribution for $N-n$ degrees of freedom. In our cases, this implies that 68% of the random data sets will give a χ^2 such that

$$\chi^2(a_1, a_2) - \chi^2(a_{1bf}, a_{2bf}) \leq 2.3. \tag{26}$$

This equation defines a closed elliptical curve around a_{1bf} and a_{2bf} in the bi-dimensional parameter space. The corresponding 1σ range of the parameter a_i is

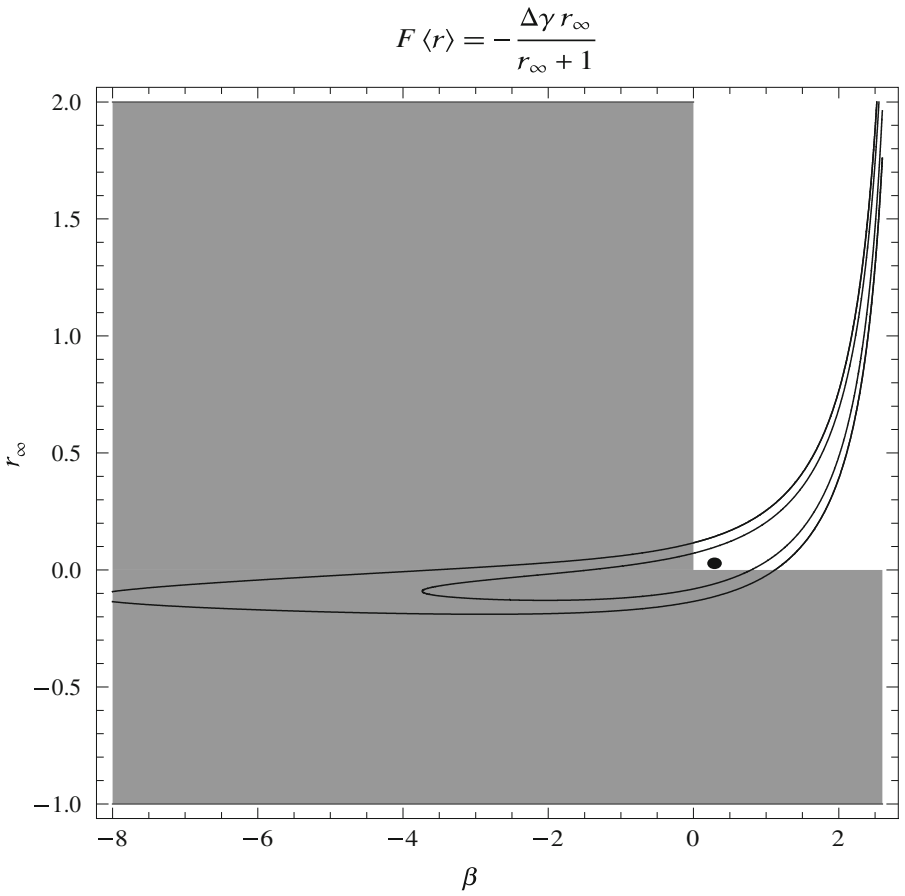

Fig. 1 Constant F: Probability ellipsis in the plane β versus r_∞. The best fit value—indicated by a *dot*—corresponds to $r_\infty = 0.0230767$ and $\beta = 0.302457$, whereas the *shady zone* represents the forbidden negative values

the range of a_i for points contained within this elliptical curve. Similarly, it can be shown that 95.4% of the random data sets will give a χ^2 such that

$$\chi^2(a_1, a_2) - \chi^2(a_{1bf}, a_{2bf}) \leq 6.17. \tag{27}$$

Again, this last equation defines an elliptical curve in parameter space and the corresponding 2σ range of each parameter a_i is the range of a_i for points contained within this elliptical curve.

The local minimum in the case of F constant is $\chi^2 = 9.02445$ for $r_\infty = 0.0230767$ and $\beta = 0.302457$. Hence, it follows from Eq. (17) with $\gamma_1 = 1$ that $\gamma_2 = 0.0800689$ and $\alpha = 0.899181$. In the F variable case, the minimum is $\chi^2 = 9.03738$ for $r_\infty = 0.0851298$ and $\gamma_2 = 0.0328392$.

In Figs. 1 and 2, we have plotted the confidence regions, that is, the sections of the elliptical curves explained above, in the β versus r_∞ plane for a constant F and in the

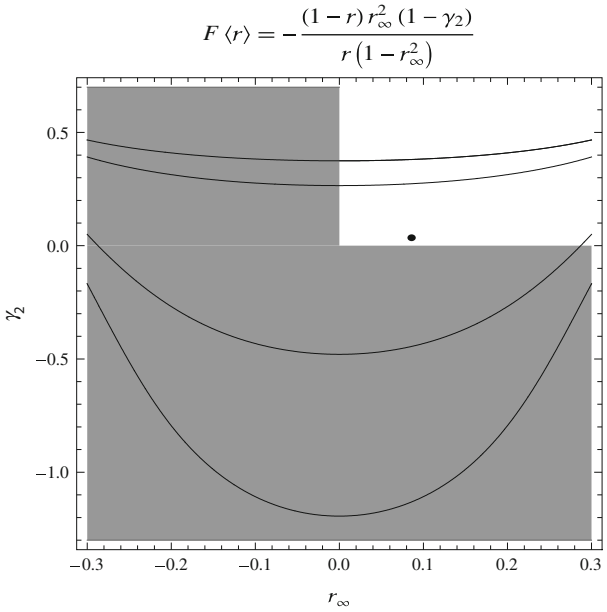

Fig. 2 Variable F: Probability ellipsis in the plane r_∞ versus γ_2. The best fit value—indicated by a *dot*—corresponds to $r_\infty = 0.0851298$ and $\gamma_2 = 0.0328392$, whereas the *shady zone* represents the forbidden negative values

r_∞ versus γ_2 plane for a variable F, respectively. The points inside the inner ellipses or between both ellipses identify the true values of parameters with 68.3 or 95.4% of probability, respectively. Also, in both figures, the best fit value for each model is represented by a dot and the shady zone means the forbidden negative values.

4 Cosmological solutions

In this section, we search for cosmological solutions of the model which was proposed in previous sections. First we analyze the density parameters which are plotted as functions of the red-shift in the left frame of Fig. 3, the straight lines corresponding to the constant $F(r)$, whereas the dashed lines to the variable $F(r)$. One can infer from this figure that the energy transfer from the dark energy to dark matter is more pronounced for the variable case, since for this case the growth of the density parameter of the dark matter and the corresponding decay of the dark energy with the red-shift are more pronounced than those for a constant $F(r)$. This behavior can also be verified from the right frame of Fig. 3 which represents the evolution of the ratio of the two energy densities $r = \rho_1/\rho_2$ with the red-shift. This last figure also shows that in the future, i.e., for negative values of the red-shift, there is no difference between the two cases, since both tend to a small value, indicating a predominance of the dark energy in the future.

In Fig. 4, the deceleration parameter $q = 1/2 + 3p/2\rho$ is plotted for the two cases. The present values of the deceleration parameter $q(0)$ and the values for the

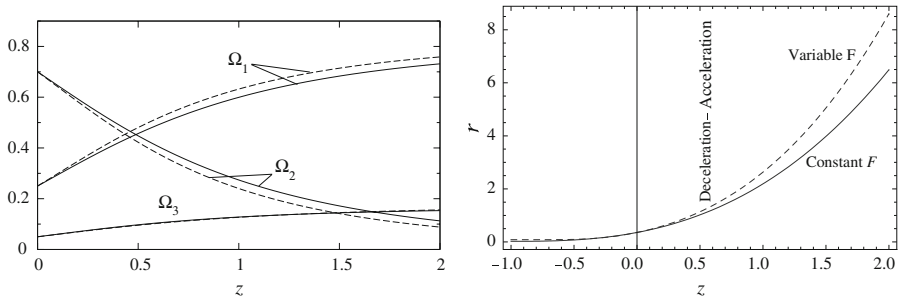

Fig. 3 *Left frame* density parameters Ω_1 (dark matter), Ω_2 (dark energy) and Ω_3 (baryons) as functions of the red-shift z; *right frame* ratio of dark matter and dark energy r as function of the red-shift z where the decelerated–accelerated transition is indicated. *Straight lines*—constant F; *dashed lines*—variable F

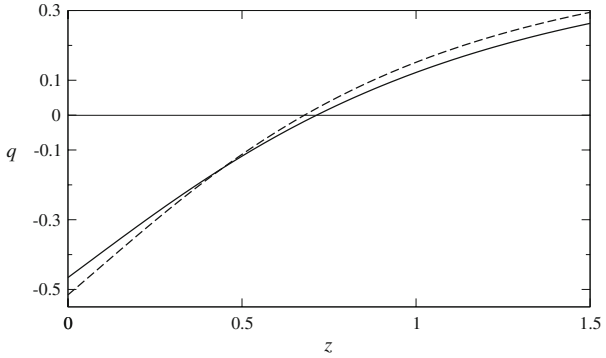

Fig. 4 Deceleration parameter q as function of the red-shift z. Constant F: indicated by a *straight line* with values $q(0) \approx -0.47$ and $z_t \approx 0.72$. Variable F: denoted by a *dashed line* with values $q(0) \approx -0.52$ and $z_t \approx 0.68$

red-shift z_t where the transition from a decelerated to an accelerated regime occur are: (i) $q(0) \approx -0.47$ and $z_t \approx 0.72$ for the constant F and (ii) $q(0) \approx -0.52$ and $z_t \approx 0.68$ for the variable F. These values are of the same order of magnitude of the observational values: $q(0) = -0.74 \pm 0.18$ (see [42]) and $z_t = 0.46 \pm 0.13$ (see [43]).

In Fig. 5, we have plotted the effective parameters w_1^e and w_2^e as functions of the red-shift z. For the variable case, one can observe that in the red-shift range $-1 \leq z \leq 2$ the effective parameters assume the values between: $-0.89 \lesssim w_1^e \lesssim 7.2 \times 10^{-4}$ and $-0.89 \lesssim w_2^e \lesssim -0.97$. Hence, in this model the effective equation of state of the dark matter constituent behaves practically as a pressureless (dust) fluid for $z > 0$ and as quintessence for $z < 0$. The dark energy in the same range behaves always as quintessence.

In Fig. 6, it is represented the difference of the apparent magnitude m and the absolute magnitude M of a source, denoted by μ_0 and whose expression is

$$\mu_0 = m - M = 5 \log \left\{ (1+z) \int_0^z \frac{dz'}{H(z')} \right\} + 25, \tag{28}$$

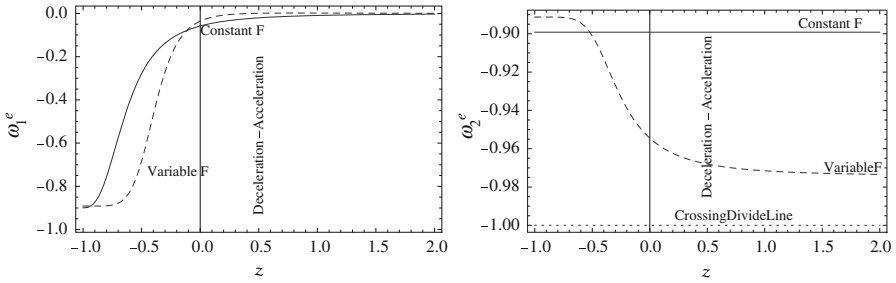

Fig. 5 Effective parameters of dark matter w_1^e and dark energy w_2^e as functions of the red-shift z. *Left frame* w_1^e; *right frame* w_2^e. The decelerated–accelerated transition is indicated in both figures. In the *right frame* is also indicated the crossing divide line to a phantom regime

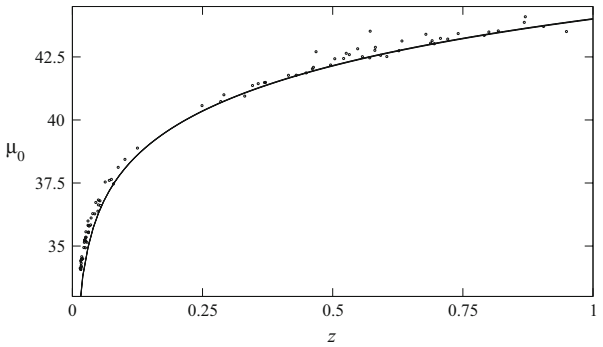

Fig. 6 Difference of the apparent and absolute magnitude μ_0 as function of the red-shift z. The *circles* are observational data for super-novae of type Ia. *Straight line* present model; *dashed line* ΛCDM model

with the quantity between braces representing the luminosity distance in Mpc. The circles in Fig. 6 are observational data for super-novae of type Ia taken from the work [44]. It is interesting to note that all μ_0—curves corresponding to the two models analyzed in the present work and the ΛCDM model practically coincide, the only small difference between them occurs for higher values of the red-shift. Furthermore, there is a good fitting of these curves with the observational data.

5 Final remarks and conclusions

As was pointed out in the introduction there exist several works in the literature on dark matter–dark energy interaction. Here we shall briefly compare our model with some other existing models.

In the work of Dalal et al. [30], the interaction term is not given explicitly, but it is proposed a phenomenological relationship $r = \rho_1/\rho_2 \propto a^{\xi}$, where the parameter ξ is adjusted with the observational data. In our case the ratio $r = \rho_1/\rho_2$ must obey the dynamical equation (9) and the possible choices for $F(r)$ follow from the study of the stability conditions of Eq. (13).

In the model proposed by Amendola et al. [31] the interaction term has the form $\delta H \rho_1$, with δ being a constant. We note that in our model the interaction term is

proportional to dark energy ρ_2 and is proportional to $H\rho_2 F(r)$ where r must obey a dynamical equation.

The interaction term of the form $\delta H\rho_1$, with δ being a constant or a function of time was also investigated by Guo et al. [32] . In the case of δ variable it was supposed that w_2 is constant. Again, in our model the interaction term is proportional to dark energy ρ_2 and w_2 is not considered to be a constant (see Fig. 5).

Recently, Böhmer et al. [33] have analyzed a model where the interaction dark matter dark energy is proportional to the energy density of the dark matter ρ_1 with three choices for the proportionality factor, namely: (i) the time derivative of the scalar field $\varphi(t)$; (ii) αH where α is a constant and (iii) a constant denoted by Γ. Here the above remarks are also pertinent.

From the analysis of the quoted works one should note that the interaction term proposed here is new, since it depends on the dark energy density and not on the energy density of dark matter. Furthermore, in the present work the ratio of the energy densities r obeys a dynamical equation whose stability analysis restricts the possible choices for $F(r)$. Due to different premisses of the quoted works, the adjustment of the parameters with the observational data is not comparable.

We may say that our model leads to a correct behavior which is expected for a viable present scenario of the Universe, by analyzing the results of last section for the deceleration parameter, density parameters and luminosity distance.

To sum up: in this work a cosmological model for the present Universe was proposed whose constituents were a non-interacting baryonic matter and interacting dark components. The interaction between the dark energy and dark matter was related to their effective barotropic indexes, which were considered as functions of the ratio of their energy densities. The energy transfer in the dark sector is proportional to the dark energy. This coupling may be motivated if one assumes that dark energy obeys standard near-equilibrium fluid thermodynamics, since according to [34] it satisfies the second law of thermodynamics and the principle of Le Châtelier. The parameters of the functions were adjusted by considering best fits to Hubble function data. Two functions were analyzed, namely, a constant and a variable one. It was shown: (i) for the proposed functions the ratio r is asymptotically stable; (ii) the energy transfer from the dark energy to the dark matter is more efficient for the variable case; (iii) for both functions the dark energy density predominates in the future; (iv) for both functions the present values of the deceleration parameter and the values of the transition decelerated/accelerated red-shift are of the same order as the observational values; (v) for the variable function, the effective ratio of the pressures and energy densities for the dark components indicates that the dark energy behaves as quintessence whereas the dark matter as practically a pressureless fluid (dust) when $z > 0$; (vi) the behavior of the parameter μ_0—related with the luminosity distance—with the red-shift does not have a sensible difference for the two functions and practically coincide with the one of the ΛCDM model, indicating a good fit with the observational values.

Acknowledgments The authors acknowledge the partial support under project 24/07 of the agreement SECYT (Argentina) and CAPES 117/07 (Brazil). LPC thanks the University of Buenos Aires for partial support under project X224, and the Consejo Nacional de Investigaciones Científicas y Técnicas under project 5169. GMK acknowledges the support by Conselho Nacional de Desenvolvimento Científico e Tecnológico (CNPq).

References

1. Riess, A.G., et al.: Observational evidence from supernovae for an accelerating universe and a cosmological constant. Astron. J. **116**, 1009 (1998)
2. Riess, A.G., et al.: BVRI light curves for 22 Type Ia Supernovae. Astron. J. **117**, 707 (1999)
3. Perlmutter, S., et al.: Measurements of omega and lambda from 42 high-redshift supernovae. Astrophys. J. **517**, 565 (1999)
4. Astier, P., et al.: The supernova legacy survey: measurement of Ω_M, Ω_Λ and w from the first year data set. Astron. Astrophys. **447**, 31 (2006)
5. Spergel, D.N., et al.: First year Wilkinson microwave anisotropy probe (WMAP) observations: determination of cosmological parameters. Astrophys. J. Suppl. **148**, 175 (2003)
6. Spergel, D.N., et al.: Wilkinson microwave anisotropy probe (WMAP) three year results: implications for cosmology. Astrophys. J. Suppl. **170**, 377 (2007)
7. Eisenstein, D.J., et al.: Detection of the baryon acoustic peak in the large-scale correlation Function of SDSS Luminous Red Galaxies. Astrophys. J. **633**, 560 (2005)
8. Sahni, V., Starobinsky, A.A.: The case for a positive cosmological lambda-term. Int. J. Mod. Phys. D **9**, 373 (2000)
9. Sahni, V.: Dark matter and dark energy. In: Papantonopoulos, E. (ed.) The physics of the early universe. Lecture Notes in Physics, vol. 653. Springer, Berlin (2005)
10. Carroll, S.M.: The Cosmological Constant. Living Rev. Rel. **4**, 1 (2001)
11. Padmanabhan, T.: Cosmological constant: the weight of the vacuum. Phys. Rept. **380**, 235 (2003)
12. Peebles, P.J.E., Ratra, B.: The cosmological constant and dark energy. Rev. Mod. Phys. **75**, 559 (2003)
13. Copeland, E.J., Sami, M., Tsujikawa, S.: Dynamics of dark energy. Int. J. Mod. Phys. D **15**, 1753 (2006)
14. Weinberg, S.: The cosmological constant problem. Rev. Mod. Phys. **61**, 1 (1989)
15. Steinhardt, P.J.: Critical Problems in Physics, In: Fitch, V.L., Marlow, D.R., Dementi, M.A.E. (eds.) Princeton University Press, Princeton (1997)
16. Chimento, L.P., Jakubi, A.S., Pavon, D.: Enlarged Q-matter cosmology. Phys. Rev. D **62**, 063508 (2000)
17. Chimento, L.P., Jakubi, A.S., Pavon, D., Zimdahl, W.: Interacting quintessence solution to the coincidence problem. Phys. Rev. D **67**, 083513 (2003)
18. Binder, J.B., Kremer, G.M.: Model for a Universe described by a non-minimally coupled scalar field and interacting dark matter. Gen. Relativ. Gravit. **38**, 857 (2006)
19. Tocchini-Valentini, D., Amendola, L.: Stationary dark energy with a baryon dominated era: solving the coincidence problem with a linear coupling. Phys. Rev. D **65**, 063508 (2002)
20. Farrar, G.R., Peebles, P.J.E.: Interacting dark matter and dark energy. Astrophys. J. **604**, 1 (2004)
21. Kremer, G.M.: Dark energy interacting with neutrinos and dark matter: a phenomenological theory. Gen. Relativ. Gravit. **39**, 965–972 (2007)
22. Huey, G., Wandelt, B.D.: Interacting quintessence, the coincidence problem and cosmic acceleration. Phys. Rev. D **74**, 023519 (2006)
23. Mangano, G., Miele, G., Pettorino, V.: Coupled quintessence and the coincidence problem. Mod. Phys. Lett. A **18**, 831 (2006)
24. Chimento, L.P., Forte, M.: Unified model of baryonic matter and dark components. Phys. Lett. B [arXiv:0706.4142] [astro-ph]
25. Cai, R.G., Wang, A.: Cosmology with interaction between phantom dark energy and dark matter and the coincidence problem. JCAP **0503**, 002 (2005)
26. Amendola, L.: Coupled quintessence. Phys. Rev. D **62**, 043511 (2000)
27. Amendola, L., Tocchini-Valentini, D.: Stationary dark energy: the present Universe as a global attractor. Phys. Rev. D **64**, 043509 (2001)
28. Amendola, L., Tocchini-Valentini, D.: Baryon bias and structure formation in an accelerating Universe. Phys. Rev. D **66**, 043528 (2002)
29. Amendola, L., Quercellini, C., Tocchini-Valentini, D., Pasqui, A.: Constraints on the interaction and self-interaction of dark energy from cosmic microwave background. Astrophys. J. **583**, L53 (2003)
30. Dalal, N., Abazajian, K., Jenkins, E.E., Manohar, A.V.: Testing the cosmic coincidence problem and the nature of dark energy. Phys. Rev. Lett. **87**, 141302 (2001)
31. Amendola, L., Camargo Campos, G., Rosenfeld, R.: Consequences of dark matter–dark energy interaction on cosmological parameters derived from SNIa data. Phys. Rev. D **75**, 083506 (2007)
32. Guo, Z.K., Ohta, N., Tsujikawa, S.: Probing the coupling between dark components of the Universe. Phys. Rev. D **76**, 023508 (2007)

33. Boehmer, C.G., Caldera-Cabral, G., Lazkoz, R., Maartens, R.: Dynamics of dark energy with a coupling to dark matter. Phys. Rev. D **78**, 023505 (2008)
34. Pavón, D., Wang, B.: Le Châtelier-Braun Principle in Cosmological Physics. Gen. Relativ. Gravit. (2008, in press)
35. Zimdahl, W., Pavon, D.: Interacting quintessence. Phys. Lett. B **521**, 133 (2001)
36. Simon, J., Verde, L., Jimenez, R.: Constraints on the redshift dependence of the dark energy potential. Phys. Rev. D **71**, 123001 (2005)
37. Abraham, R.G., et al.: The Gemini deep deep survey: I. Introduction to the survey, catalogs and composite spectra. Astron. J. **127**, 2455 (2004)
38. Treu, T., Stiavelli, M., Moller, P., Casertano, S., Bertin, G.: The properties of field elliptical galaxies at intermediate redshift. II: photometry and spectroscopy of an HST selected sample. Mon. Not. R. Astron. Soc. **326**, 21 (2001)
39. Nolan, P.L., Tompkins, W.F., Grenier, I.A., Michelson, P.F.: Variability of EGRET gamma-ray sources. Astrophys. J. **597**, 615 (2003)
40. Press, W.H., et al.: Numerical Recipes. Cambridge University Press, Cambridge (1997)
41. Freedman, W.L., et al.: Final results from the Hubble Space Telescope key project to measure the Hubble constant. Astrophys. J. **553**, 47 (2001)
42. Virey, J.M., et al.: Determination of the deceleration parameter from supernovae data. Phys. Rev. D **72**, 061302(R) (2005)
43. Riess, A.G., et al.: Type Ia Supernova discoveries at $z > 1$ from the Hubble Space Telescope: evidence for past deceleration and constraints on dark energy evolution. Astrophys. J. **607**, 665 (2004)
44. Riess, A.G., et al.: New Hubble Space Telescope discoveries of type Ia supernovae at $z > 1$: narrowing constraints on the early behavior of dark energy. Astrophys. J. **659**, 98 (2007)